Pore-Diffusion Mechanisms during Vapor-Phase Adsorption

EDWARD J. NEMETH and EDWARD B. STUART

University of Pittsburgh, Pittsburgh, Pennsylvania

The mechanism of diffusion in an absorbent pore was studied by applying adsorption rate data to the Damköhler equation. Most of the data were taken in the multimolecular region of the nitrogen-silica gel adsorption isotherm. Vapor-phase and adsorbed-phase contributions to the total transport were separated. Vapor-phase transport increased with temperature and was most dominant at relative pressures of 0.4 to 0.6. Adsorbed-phase diffusivities were of the order of 10^{-2} — 10^{-3} sq. cm./sec. and showed some dependence on the amount adsorbed at surface coverages greater than 1.5 molecular layers.

The diffusion of the molecule into the pore space of an adsorbent is the rate controlling step during the adsorption process. The adsorption equilibrium of the exposed surface with the vapor is established nearly instantaneously (1). The diffusion into the pore of an adsorbent takes place either by diffusion in the vapor phase or by migration of the adsorbed molecules. A particular molecule will diffuse by each mechanism, since it continually adsorbs and desorbs during its time in the pore. However, some molecules are, at any particular instant, always diffusing in the vapor space, and some are diffusing in the adsorbed layer. Therefore, we can discuss the vapor-phase diffusion and adsorbed-phase diffusion as related but separate entities.

With a few exceptions (2, 3), most of the pore-diffusion measurements and analyses have considered only gas-phase diffusion or diffusion over the adsorbing surface by less than a monomolecular layer. The adsorbed-phase diffusion then is usually described by two-dimensional gas dynamics or by an activated mechanism by which the molecule moves from one surface site to another. However, in the multimolecular adsorption region, the adsorbed film assumes a liquidlike character, and diffusion further into the pore probably occurs by movement of the molecules over each other (4, 5). Testin and Stuart (2) have shown that this diffusion is similar to liquid-phase diffusion.

The purpose of this work is to study the mechanism of pore diffusion during multimolecular adsorption.

MATHEMATICAL MODEL

Damköhler (6) first presented an accurate analysis of the mechanisms which control adsorption rates. His model included the effects of both vapor- and adsorbed-phase diffusion and is used here.

In the vapor phase of the pore, the diffusion process can be described by Fick's law in the form (7)

$$\frac{\partial}{\partial x}\left(D_v \frac{\partial C_v}{\partial x}\right) = \frac{\partial[(K+1)C_v]}{\partial \theta} \tag{1}$$

where

$$K = \frac{n_{v-a}}{n_v} \tag{2}$$

and represents the fraction of the molecules which leave the vapor phase to enter the adsorbed phase. Suitable boundary and initial conditions for Equation (1) are

$$\begin{aligned} x &= 0 & C_v &= C_v^0 \\ x &= L & \frac{\partial C_v}{\partial x} &= 0 \\ \theta &= 0 & C_v &= 0 \end{aligned}$$

where L refers to the effective diffusional path length. Then the solution to (1) for constant K and D_v is

$$\frac{C_v}{C_v^0} = 1 - \frac{4}{\pi}\sum_{m=1}^{\infty}\left(\frac{1}{2m-1}\right) \exp\left[-(2m-1)^2 \frac{\pi^2 D_v \theta}{(1+K)4L^2}\right] \sin\left[(2m-1)\frac{\pi x}{2L}\right] \tag{3}$$

At any time θ, the total mass which has penetrated the pore is given by

$$n = \int_0^\theta D_v A_v \frac{\partial C_v}{\partial x}\bigg|_{x=0} d\theta + \int_0^\theta D_a A_a \frac{\partial C_a}{\partial x}\bigg|_{x=0} d\theta \tag{4}$$

Now, assuming an instantaneous establishment of equilibrium between the vapor and adsorbed phase, we get

$$A_a \frac{\partial C_a}{\partial x} = A_v \frac{\partial (A\, C_v)}{\partial x} \tag{5}$$

where $A = n_a/n_v$. Then, for constant A

$$n = \frac{8\, L\, C_v^0\, A_v\, (D_v + A\, D_a)(1+K)}{\pi^2\, D_v}\left\{\frac{\pi^2}{8} - \sum_{m=1}^{\infty}\frac{1}{(2m-1)^2}\exp\left[\frac{-(2m-1)^2\,\pi^2\, D_v\,\theta}{(1+K)\,4\,L^2}\right]\right\} \tag{6}$$

The mass of adsorbate taken up by the pore is usually expressed as a volume of vapor per gram of adsorbent at STP. Thus, Equation (6) becomes

$$V_a = \frac{273.2\,P}{Z\,T}\,\frac{8\,C_v^0\,V_P\,(D_v + A\,D_a)(1+K)}{\pi^2\,D_v}\left\{\frac{\pi^2}{8} - \sum_{m=1}^{\infty}\frac{1}{(2m-1)^2}\exp\left[\frac{-(2m-1)^2\,\pi^2\,D_v\,\theta}{(1+K)\,4\,L^2}\right]\right\} \tag{7}$$

Then, by using the definition $\Phi = V_a/V_{a,eq}$

$$\Phi = 1 - \frac{8}{\pi^2}\sum_{m=1}^{\infty}\frac{1}{(2m-1)^2}\exp\left[\frac{-(2m-1)^2\,\pi^2\,D_v\,\theta}{4\,L^2\,(1+K)}\right] \tag{8}$$

Edward J. Nemeth is with Applied Research Laboratory, United States Steel Corporation, Monroeville, Pennsylvania.

The form of K is necessary to complete (8). By taking a mass balance over a differential element of pore length, the value of n_{v-a} can be determined. Thus

$$n_{v-a} = \int_0^\theta \left[D_v A_v \frac{\partial C_v}{\partial x} \bigg|_{x+\Delta x} - D_v A_v \frac{\partial C_v}{\partial x} \bigg|_x \right] d\theta - n_v \quad (9a)$$

$$n_{v-a} = A\, n_v - \int_0^\theta \left[D_a A_a \frac{\partial C_a}{\partial x} \bigg|_{x+\Delta x} - D_a A_a \frac{\partial C_a}{\partial x} \bigg|_x \right] d\theta \quad (9b)$$

By substituting (5) in (9a) and by assuming constant A and D_a, the integral terms can be eliminated in (9a) and (9b) and n_{a-v} determined. Using (2), then, we get

$$K = \frac{D_v (1 + A)}{D_v + A\, D_a} - 1 \quad (10)$$

and (8) becomes the Damköhler equation in the form

$$\Phi = 1 - \frac{8}{\pi^2} \sum_{m=1}^{\infty} \frac{1}{(2m-1)^2} \exp \left[\frac{-(2m-1)^2 \pi^2 (D_v + A\, D_a)}{4 L^2 (1 + A)} \theta \right] \quad (11)$$

The quantity A is not always constant. Therefore, (11) is strictly applicable to Henry's law adsorption isotherms. Further, even among those adsorption systems which do exhibit the behavior demanded by (11), the adsorbed-phase diffusivity varies with the concentration on the surface (*4, 5, 8, 9*) enough so that the assumption of a constant value of K in (8) is probably not valid. At higher values of surface coverage, approaching or in the multimolecular adsorption region, the diffusion coefficient of the adsorbed phase has been shown to approach a constant value (*2, 10*) independent of surface coverage. The value of A often shows little variation here also. For some types of adsorption isotherms, notably the type IV isotherm, the value of A is often nearly a linear function of reduced pressure over some range of the multimolecular adsorption. Thus, A can be expressed (*7*) as

$$A = A_0 + \frac{B}{P} \quad (12)$$

in this region. Using (12) to solve for an equivalent form of (11), we get

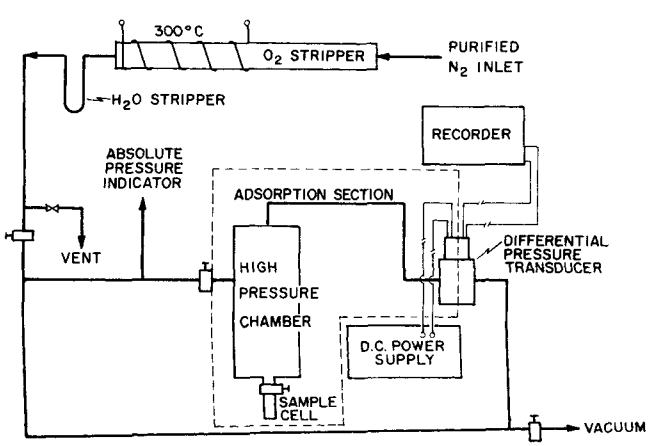

Fig. 1. Equipment schematic.

Table 1. Adsorbent Properties
Davison Grade 70 silica gel

Particle size	−50 mesh, +60 mesh
Average particle diameter	0.0276 cm.
Pore volume/g. of adsorbent	1.05 ml.
Surface area/g. of adsorbent	253 sq.m.
Average pore radius	82.5Å
Range of pore radii	<10 to 120Å

$$\Phi = 1 - \frac{8}{\pi^2} \sum_{m=1}^{\infty} \frac{1}{(2m-1)^2} \exp \left[\frac{-(2m-1)^2 \pi^2 (D_v + A_0\, D_a)}{4 L^2 (1 + A_0)} \theta \right] \quad (13)$$

Therefore, for the limited, essentially linear, region of a multimolecular adsorption isotherm, (13) could provide an accurate description of the physical adsorption process if the possibility of a constant D_a is realized.

The ratio of the vapor- and adsorbed-phase contribution to the total pore diffusion can be given by

$$\frac{N_v}{N_a} = \frac{K+1}{A-K} = \frac{D_v}{A\, D_a} \quad (14)$$

The vapor-phase diffusivity can be calculated from either the Knudsen-diffusion relationship or from the applicable bulk-diffusion relationship (*11* to *13*). Therefore, if a means for establishing L can be obtained, the contributions of the vapor and adsorbed phase to the total transport into the pore can be determined.

EXPERIMENTAL

Apparatus and Procedure

The stainless steel apparatus is illustrated in Figure 1.

The adsorbent was Davison Grade 70 silica gel. Its physical properties are shown in Table 1. Surface areas and pore volumes were measured by the B.E.T. method. The adsorbate in all cases was prepurified nitrogen treated to remove any trace oxygen or water contamination. The silica gel in the

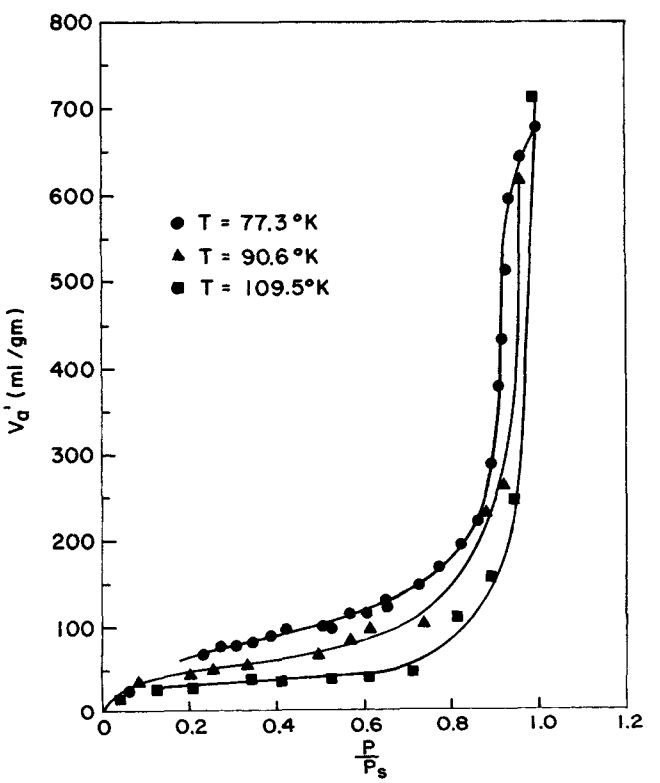

Fig. 2. Equilibrium isotherms.

TABLE 2

Temperature, °K.	$D_a/L^2 \times 10^3$ sec.$^{-1}$
90.6	0.41
109.5	1.8

sample chamber was degassed before each run at 300°C. and 10^{-4} mm. Hg pressure for at least 1 hr.

The sample chamber was capable of being isolated from the rest of the system. Nitrogen was admitted to the entire system, except to the sample chamber, to some predetermined pressure. The sample was previously cooled to the desired temperature. The valve separating the adsorption and reference pressure sides was closed, and adsorption rate measurements were initiated by opening the valve to admit nitrogen to the sample chamber. A continuous strip chart recording of the pressure differential between the reference and adsorption sides of the equipment was then used to determine the adsorption rate. In all cases, the difference in pressure between the beginning and end of the adsorption time did not produce a significant change in relative pressure.

Data

The volume of nitrogen in the adsorbent pore is calculated by

$$V_a = \frac{273.2\ \Delta P}{760\ W_g}\left[\frac{V_P}{T_R} + \frac{V_s - \dfrac{W_g}{\rho_g}}{T}\right] \qquad (15)$$

where ΔP refers to the pressure difference at a time during the run and the start of the run. The term V_a then indicates the total quantity in the pore, both adsorbed and vapor phases. Then

$$V_a = V_a' + V_v \qquad (16)$$

By using the liquid nitrogen density (*14*) of 0.808 cc./g., the volume of the pore taken up by the adsorbed molecules is $1.549 \times 10^{-3}\ V_a'$. This quantity must be subtracted from the empty pore volume to obtain the pore volume occupied by the vapor phase. Then, with the appropriate algebraic manipulation

$$V_a' = \frac{V_a - V_{pe}\left(\dfrac{273.2°\text{K.}}{1\text{ atm.}}\dfrac{P}{T}\right)}{1 - 1.549 \times 10^{-3}\left(\dfrac{273.2°\text{K.}}{1\text{ atm.}}\dfrac{P}{T}\right)} \qquad (17)$$

Equation (17) can be used therefore to calculate the adsorption isotherms by using the pressure difference between the start and conclusion of the run. The isotherms for 77.3°, 90.6°, and 109.5°K. are shown in Figure 2. The linear regions of these isotherms extend from about $P/P_s = 0.1$ to about $P/P_s = 0.6$.

While (17) is applicable to only equilibrium data, (15) can be used to give the quantity of adsorbate in the pore at any time. Figures 3 and 4 show data for 90.6° and 109.5°K. adsorption runs.

CALCULATIONS

Effective Diffusivities

Equation (11) can be applied to the experimental data to obtain diffusivity values. If the diffusional path length L is taken as the radius of the particle, an effective diffusivity, defined by

$$D_e = \frac{D_v + A\ D_a}{1 + A} \qquad (18)$$

can be calculated.

The best way to fit data to (11) is to take advantage of the rapid convergence of the series terms. By using τ to represent all the terms in the exponent exclusive of θ and the summation index, only the first term of the series is significant for $\Phi \geq 0.4$. All the data indicate that Φ reaches

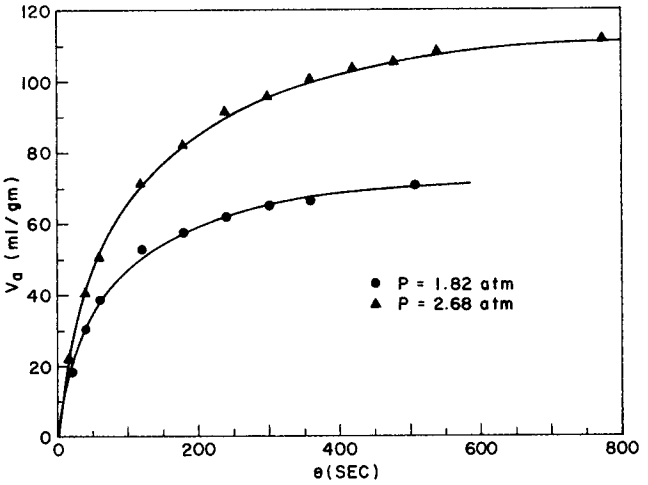

Fig. 3. Rate data at 90.6°K.

0.4 before one-tenth of the entire run is completed. Therefore, limiting the analysis to $\Phi \geq 0.4$ does not seriously limit the scope of the data. Equation (11) can be written then as

$$1 - \Phi = \frac{8}{\pi^2}\, e^{-\tau\theta} \qquad (19)$$

and the data are amenable to semilogarithmic representation. Figures 5 and 6 show data plotted in this way.

Other curve fitting techniques are possible to analyze the complete range of Φ, but the values of τ are not significantly different (*7*).

Vapor-Phase Diffusivity

The value of D_v must be obtained to be able to find the value of D_a. For the pore sizes and range of nitrogen pressures considered here, some of the data, especially at the higher pressures, would not be expected to be in the Knudsen flow regime but in some transition region. The Knudsen numbers (λ/r) based on the average pore radius range from 0.25 to 10.5. Therefore, some interpolation formulas (*11, 12, 15*) might be expected to apply. The bulk diffusion mechanism is excluded from consideration because only one adsorbate, nitrogen, was present in the sample chamber. Only Knudsen diffusion and Poiseuille flow into the pore therefore need be considered. For the high pressure runs, where Poiseuille flow is likely to be important, the vapor-phase flow diameter is diminished by the adsorbate on the pore surface, thus increasing the probability of Knudsen diffusion. Further, the shapes of the curves show more dependency on relative pressure than on absolute pressure. Since the Knudsen diffusivity is independent of absolute pressure, it seems likely then that Knudsen flow dominates the vapor process. However, even if Poiseuille flow is a larger contributor than reasoned here, no substantial error in the value of D_v would be involved in using the Knudsen diffusivity rather than the Poiseuille relationship because the Knudsen diffusion coefficient and the coefficient calculated by forcing the Poiseuille equation into a Fick's law form both result in calculated diffusivities of the order of magnitude of 10^{-2} sq.cm./sec. For instance, at $T = 109.5$°K., $P = 13.6$ atm., and $r = 82.5$Å, the Poiseuille diffusivity is 1.26×10^{-2} sq.cm./sec. and the Knudsen diffusivity is 1.60×10^{-2} sq.cm./sec. Therefore, the Knudsen diffusivity is used to calculate D_v.

Effective Diffusional Path Length

The assumptions made in this calculation are as follows:

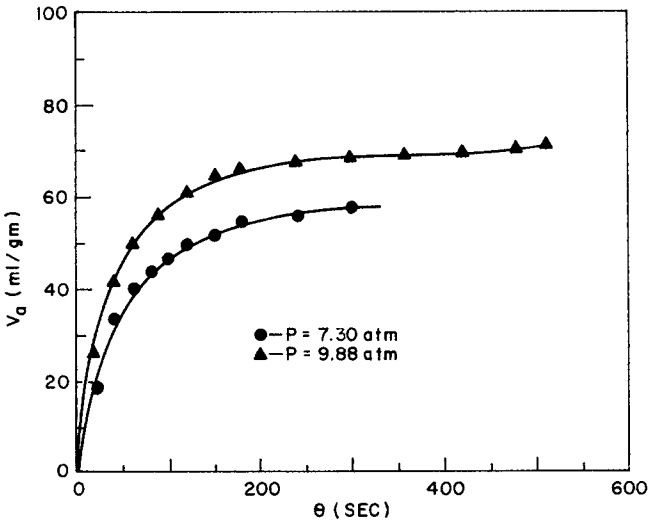

Fig. 4. Rate data at 109.5°K.

1. For the runs at or very near the saturation pressure, all the diffusion into the pore takes place in the adsorbed phase. The vapor phase is essentially excluded from the pore by a buildup of an equilibrium multimolecular layer at the mouth or the pore.

2. The adsorbed phase diffusivity does not change for $V_a' \geqq 150$ ml./g. The exposed surface is energetically uniform (*1*) as indicated by the fact that the heat of adsorption is not a function of surface coverage above $V_a' \geqq 150$ ml./g. (*7*). The uniform energies at the surface would allow the adsorbed molecule to diffuse at a constant surface potential.

3. The same value of L applies for the vertical leg of the adsorption isotherm as for adsorption in other regions.

The value of A varies significantly throughout the time of adsorption owing to the large increase in surface coverage in the pore throughout the course of the adsorption for $V_a' \geqq 150$ ml./g. An effective value of A must then be considered to evaluate L in the high coverage region of the isotherm. Using (7) for this region of the isotherm, we can write for $\Phi \geqq 0.4$

$$\frac{dV_a}{d\theta} = \frac{2\,(273.2)\,PV_P\,(D_v + A\,D_a)}{Z\,T\,L^2} \exp \left[\frac{-\,(D_v + A\,D_a)\,\pi^2}{4\,L^2\,(1+A)}\,\theta \right] \quad (20)$$

and define

$$b = \frac{2\,(273.2)\,PV_P\,(D_v + A\,D_a)}{Z\,T\,L^2} \quad (21)$$

The expression given by (21) contains D_a, A, and L^2 as unknowns. The term D_a/L^2 can be found from the slope of data plotted as in Figures 5 and 6 for the runs at saturation, D_v can be calculated from the expression for the Knudsen diffusion coefficient, and b can be obtained from the intercept of a semilogarithmic plot of $dV_a/d\theta$ vs. θ. The slope of the line of the semilogarithmic plot of $dV_a/d\theta$ vs. θ should be the same as the slope of the semilogarithmic plot of $(1-\Phi)$ vs. θ and is again called τ. Thus, for the rate data where $V_a' > 150$ ml./g., eliminating A from the τ and b experimental values, we get

$$L^2 = \frac{D_v}{\frac{b\,Z\,T}{2(273.2)\,PV_P}\left[1 + \frac{(D_a/L^2)\,\pi^2}{4\tau}\right] + \left(\frac{D_a}{L^2}\right)} \quad (22)$$

The pertinent D_a/L^2 data are tabulated in Table 2.

The most suitable value of r to be used for the calculation of the vapor diffusivity is the average pore radius corrected for the amount adsorbed on the walls. Therefore, the value of L will be dependent on the B.E.T. data and will add another piece of information to the B.E.T. data.

The slopes of the lines plotted from the $dV_a/d\theta$ data agree with the τ values for the $1-\Phi$ data within experimental error. The average value is used to calculate L. The results are shown in Table 3.

Table 3

Temp., °K.	V_a', ml./g.	P, atm.	$\frac{-dV_a}{d\theta} \times 10^3$, ml./g.-sec.	b	$\tau \times 10^3$, sec.$^{-1}$	$\frac{L}{R_P}$
109.5	158	12.39	8.74	0.82	7.5	109
109.5	246	13.05	6.15	0.74	8.3	122
90.6	264	3.34	1.25	0.29	1.7	104

Table 4. Diffusion Coefficients at 90.6°K.

Equilibrium pressure, atm.	P/P_s	V_a', ml./g.	$D_e \times 10^6$, sq.cm./sec.	$D_a \times 10^2$, sq.cm./sec.
0.320	0.0883	33.0	1.3	1.7
0.747	0.224	43.0	1.3	1.7
0.948	0.284	48.2	1.2	1.5
1.21	0.334	54.7	1.2	1.4
1.82	0.503	65.5	0.6	0.60
2.07	0.572	74.9	0.6	0.60
2.23	0.616	96.8	0.4	0.38
2.68	0.743	103.0	0.4	0.40
3.18	0.878	231.0	0.2	0.096
3.34	0.922	264.0	0.1	0.096
3.46	0.955	616.0	0.08	0.096

One monolayer, determined by B.E.T. method, contains 39.1 ml./g.

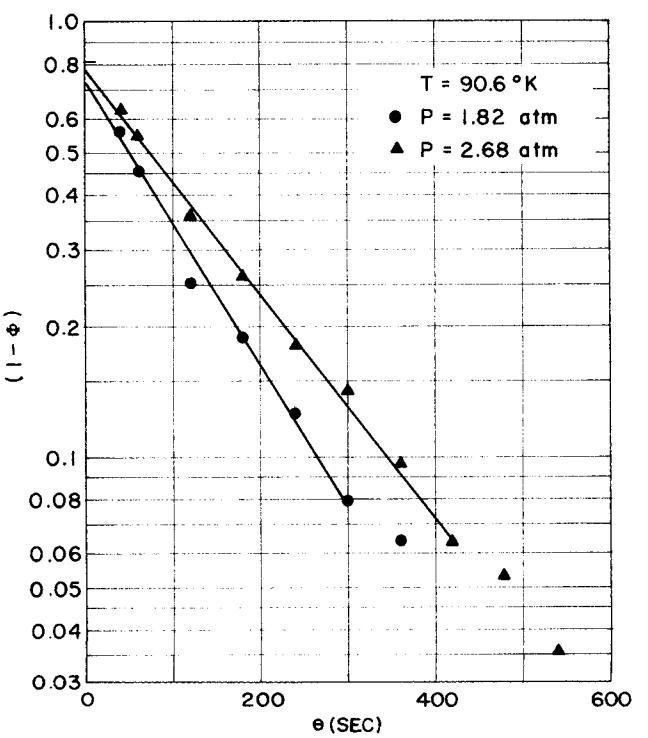

Fig. 5. Rate analysis according to Equation (19) for the determination of τ at 90.6°K.

TABLE 5. DIFFUSION COEFFICIENTS AT 109.5°K.

Equilibrium pressure, atm.	P/P_s	V_a', ml./g.	$D_e \times 10^6$, sq.cm./g.	$D_a \times 10^2$, sq.cm./g.
0.571	0.041	16.4	1.5	1.3
0.947	0.068	26.0	0.9	0.83
1.71	0.123	28.3	0.5	0.49
2.90	0.209	28.4	1.1	1.0
4.79	0.345	36.1	1.0	0.90
5.72	0.413	35.9	1.2	1.2
7.30	0.526	40.1	1.2	1.2
8.54	0.615	43.0	1.1	1.0
9.88	0.712	47.6	1.1	1.0
11.17	0.806	110.0	0.7	—
12.39	0.892	158.0	0.6	0.42
13.05	0.942	246.0	0.3	0.42
13.68	0.985	717.0	0.3	0.42

One monolayer, determined by B.E.T. method, contains 29.5 ml./g.

Absorbed-Phase Diffusion Coefficients

By using the average value of L, 112 R_P, the adsorbed-phase diffusion coefficients are calculated. These are tabulated in Tables 4 and 5 along with the effective diffusivities.

Contributions of the Vapor and Adsorbed Phase

By Equation (14) we can calculate the contribution of the vapor and adsorbed phase to the total transport into the pore. This is shown in Figure 7. The data at 77.3°K. ($T/T_c = 0.611$) are taken from Testin and Stuart (2). All of the curves bend downward sharply near saturation because A is increasing sharply here and approaching infinity at saturation.

DISCUSSION

The adsorbed-phase diffusivity is not a function of surface coverage in the region of about 1 to 1.5 monolayers surface coverage. The behavior of the adsorbed-phase diffusivity below monolayer coverage is uncertain, but the diffusivity is not so different from that above monolayer adsorption that the possibility of the two being the same should be discounted. The values of the adsorbed-phase diffusivities are of the order of magnitude of 10^{-2} sq.cm./sec., the same order of magnitude as gas-phase coefficients. This value of D_a is higher than most surface diffusivity values reported for less than monolayer surface coverage. For instance, Schneider and Smith (8) tabulate various surface diffusivity values in the range of 10^{-3} to 10^{-6} sq.cm./sec. for <1 to 95% monolayer coverage. It seems reasonable that the adsorbed layer becomes fluid enough to lead to higher diffusion coefficients in the multimolecular region. Temperature effects on the adsorbed-phase diffusivities are minimal. Therefore, the diffusion mechanism is not one in which the molecules require an activation energy for movement. In the multimolecular region where coverages become greater than 1.5 monolayers, the adsorbed-phase diffusion coefficient apparently decreases as predicted by Gilliland et al. (5) and continues to decrease in the capillary condensation portion of the isotherm. The adsorbed-phase diffusivity is temperature dependent in the capillary condensation region, and the activation energy is nearly the same value as the heat of liquefaction (7) at this point. Evidently, self-interference of adsorbed molecules hinders diffusion at high coverages.

From Figure 7 it can be seen that the vapor-phase contribution to the overall transport in the pore is more dominant in the middle region of the relative pressure range and increases in dominance as the temperature increases. In both of these cases, the equilibrium in the pore is more favorable to the vapor phase. Therefore, the concentration gradient in the vapor phase relative to the adsorbed phase is greater in these regions, and more movement of vapor molecules is promoted. Krasuk and Smith (16), by working with the data of Miller and Kirk (17), noted the opposite effect of temperature on the surface contribution to the overall transport in the pore for ethanol, 1-propanol, and 1-butanol. However, in their case the temperature was high enough so that the surface coverage was much less than 1 monolayer, and an activated surface-diffusion mechanism probably prevailed. Thus, it would seem that for very low surface coverage (corresponding to P/P_s very

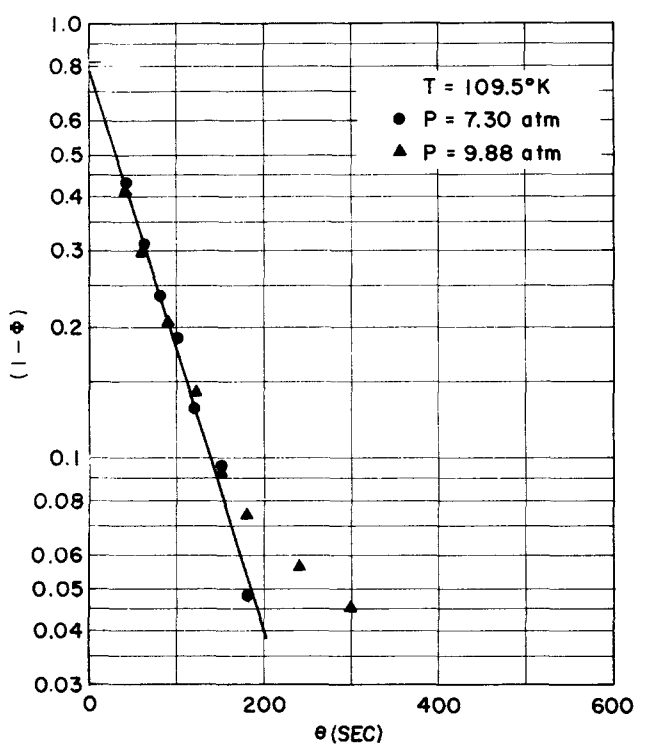

Fig. 6. Rate analysis according to Equation (19) for the determination of τ at 109.5°K.

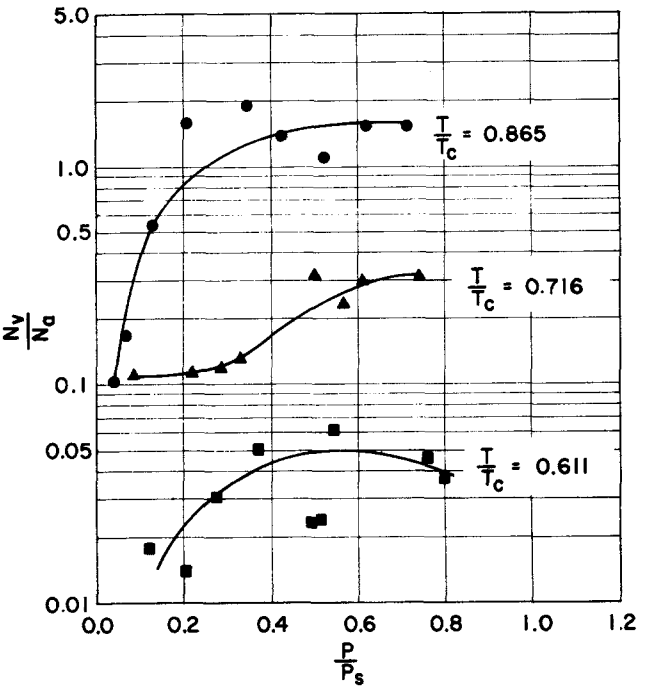

Fig. 7. Comparison of vapor- and surface-phase transport.

small), the trend of the curves in Figure 7 would be downward with possible crossover of the lines.

All of the data presented here are dependent on the accuracy of the B.E.T. surface characterization data and, of course, the model chosen. While the values calculated from the B.E.T. isotherm obviously are not exact physical descriptions, they do provide a realistic approximation, and the vapor diffusion coefficients should be exact within ± 30% (*18*). Because the data fit the shape of the curve predicted by the Damköhler equation, the model appears accurate. The consideration of constant parameters for the integrations involved in the derivations of the equations means that the calculated values are averages over some range of surface coverage but are accurate in order of magnitude.

The rate curves all exhibit a slower approach to equilibrium at high Φ (Figures 3 to 6) than predicted by the Damköhler equation. This is probably because the heat of adsorption causes local high temperatures on the pore surface and thus shifts the equilibrium temporarily. Also, the diffusion into the smaller pores is slower, and the tailing off of the rate curves could reflect this.

CONCLUSIONS

The Damköhler analysis of adsorption kinetics has been applied successfully to the multimolecular adsorption range of the type IV adsorption isotherm. The contributions of the vapor and adsorbed phases to the total transport in the pore have been separated. Vapor-phase transport contribution increases with temperature and also increases in the middle range of the reduced pressures.

The effective length of travel in the pore of the molecule has been calculated to be 112 times the particle radius for this system. Adsorbed-phase diffusivities are $10^{-2} - 10^{-3}$ sq.cm./sec. order of magnitude. These are relatively constant for the range 1.0 to 1.5 monolayer coverage but decrease in the higher coverage region.

ACKNOWLEDGMENT

This work was supported by the National Aeronautics and Space Administration Grant No. NSG(T)-70.

NOTATION

A = ratio of the number of moles in the pore-space vapor phase to the number of moles in the adsorbed phase, dimensionless
A_a = area normal to the direction of diffusion in the adsorbed phase, cm.
A_v = area normal to the direction of diffusion in the vapor phase, sq.cm.
A_0 = constant in the equation for A in the linear region of the isotherm, dimensionless
b = defined by (21)
B = constant in the equation for A in the linear region of the isotherm, atm.
C_a = adsorbed-phase concentration, moles/sq.cm.
C_v = vapor-phase concentration, moles/ml.
C_v^0 = constant vapor-phase concentration in the occluded vapor, moles/ml.
D_a = adsorbed-phase diffusivity, sq.cm./sec.
D_v = vapor-phase diffusivity, sq.cm./sec.
K = distribution coefficient defined as the ratio of the number of moles leaving the vapor phase to the number of moles which diffuse in the phase, dimensionless
L = effective diffusional path length, cm.
M = molecular weight
m = summation index
n = total number of moles which diffuse into the pore, moles
n_a = number of moles in the adsorbed phase
$\overline{n_v}$ = number of moles in the pore-space vapor phase
n_{v-a} = number of moles which enter the adsorbed phase from the vapor phase
N_a = mass which diffuses in the adsorbed phase, moles
N_v = mass which diffuses in the vapor phase, moles
P = pressure, atm.
P_s = saturation pressure, atm.
r = capillary radius, Å
R = gas constant
R_P = particle radius, cm.
T = sample temperature, °K.
T_c = critical temperature, °K.
T_R = room temperature, °K.
V_a = total mass in the adsorbent pore converted to volume per gram of adsorbent at STP, ml./g.
$V_{a,eq}$ = total mass in the adsorbent pore at equilibrium converted to volume per gram of adsorbent at STP, ml./g.
V_a' = total mass on the adsorbent surface converted to volume per gram of adsorbent at STP, ml./g.
V_v = total mass in the pore-space vapor phase converted to volume per gram of adsorbent at STP, ml./g.
V_P = pore volume, ml./g.
V_{pe} = empty pore volume, ml./g.
V_s = sample cell volume, ml./g.
W_g = weight of silica gel sample, g.
x = axial dimension of the pore, cm.
Z = compressibility factor

Greek Letters

θ = time, sec.
ρ_g = silica gel density, g./ml.
λ = mean free path, Å.
Φ = fractional approach to equilibrium, dimensionless
τ = exponent in Damköhler equation, sec.$^{-1}$

LITERATURE CITED

1. de Boer, J. H., "The Dynamical Character of Adsorption," Clarendon Press, Oxford, England (1953).
2. Testin, R. F., and E. B. Stuart, *Chem. Eng. Progr. Symposium Ser. No. 74*, **63**, 10 (1966).
3. Babbitt, J. P., *Can. J. Res.*, **28A**, 449 (1950).
4. Dacey, J. R., *Ind. Eng. Chem.*, **57**, 26 (1965).
5. Gilliland, E. R., R. F. Baddour, and J. L. Russell, *AIChE J.*, **4**, 90 (1958).
6. Damköhler, G., *Z. Physik. Chem.*, **174**, 222 (1935).
7. Nemeth, E. J., Ph.D. thesis, Univ. Pittsburgh, Pa. (1967).
8. Schneider, Peter, and J. M. Smith, *AIChE J.*, **14**, 886 (1968).
9. Smith, R. K., and A. B. Metzner, *J. Phys. Chem.*, **68**, 2741 (1964).
10. Carman, R. C., and F. A. Raal, *Trans. Faraday Soc.*, **50**, 842 (1954).
11. Scott, D. S., and F. A. L. Dullien, *AIChE J.*, **8**, 113 (1962).
12. Rothfeld, L. B., *ibid.*, **9**, 19 (1963).
13. Cunningham, R. S., and C. J. Geankoplis, *Ind. Eng. Chem. Fundamentals*, **4**, 535 (1968).
14. Emmett, P. H., and S. Brunauer, *J. Am. Chem. Soc.*, **59**, 1553 (1937).
15. Evans, R. B., G. M. Watson, and E. A. Mason, *J. Chem. Phys.*, **36**, 1894 (1962).
16. Krasuk, J. H., and J. M. Smith, *Ind. Eng. Chem. Fundamentals*, **4**, 102 (1965).
17. Miller, D. N., and R. S. Kirk, *AIChE J.*, **4**, 90 (1958).
18. Wheeler, A., "Advances in Catalysis," Vol. III, Academic Press, New York (1951).

Manuscript received March 15, 1968; revision received April 21, 1969; paper accepted April 23, 1969.